Efficient Data Assimilation for High-Dimensional Geophysical Systems: A Local Unscented Transform Kalman Filter

Kwangjae Sung

Introduction

This paper proposes an efficient data assimilation approach based on the sigma-point Kalman filter (SPKF). With a potential for high-dimensional nonlinear filtering applications, the proposed approach, designated as the local unscented transform Kalman filter (LUTKF), is similar to the SPKF in that the mean and covariance of the nonlinear system are estimated by propagating a set of sigma points—also referred to as ensemble members—generated using the scaled unscented transformation (SUT), while making no assumptions with regard to nonlinear models. The LUTKF offers the following advantages over the SPKF:

- The use of the non-augmented state makes it easier to implement the localization scheme at each model grid point by considering only the original model state, not including the process and measurement noises in the state vector, and it allows the LUTKF to be more computationally feasible for high-dimensional systems by reducing the number of sigma points
- Unlike the SPKF, the LUTKF can employ the localization method used to enhance the computational efficiency and to suppress spurious correlations between distant locations in the error covariance matrix, thus, it is computationally feasible with a small number of the sigma points for high-dimensional systems and can provide accurate and reliable analysis results.

SPKF

The basic framework for the SPKF algorithm involves estimating the state of nonlinear system by the dynamical model and the observation model with non-additive noise as follows:

$$\mathrm{x}_k = f(\mathrm{x}_{k-1}, \mathrm{w}_{k-1}), \tag{1}$$
$$\mathrm{z}_k = h(\mathrm{x}_k, \mathrm{v}_k), \tag{2}$$

where x_k denotes the system state vector at time k, $f(\cdot)$ is the and measurement noises are treated as specific states to be estimated; however, they are not actually estimated using the filter. Hence, the state vector nonlinear function of the state, z_k is the measurement vector, and $h(\cdot)$ is the nonlinear function that describes the relationship between the measurement and state. The process noise w_k and measurement noise v_k are assumed to be white noise and uncorrelated with the zero-mean and covariance matrices Q_k and R_k, respectively. In the SPKF, the process for the SPKF is redefined as the concatenation of the original state, process noise, and measurement noise. The augmented state vector x_k^a and corresponding covariance P_k^a are given by

$$\mathrm{x}_k^a = [\mathrm{x}_k^T \quad \mathrm{w}_k^T \quad \mathrm{v}_k^T]^T, \tag{3}$$
$$P_k^a = \begin{bmatrix} P_k & 0 & 0 \\ 0 & Q_k & 0 \\ 0 & 0 & R_k \end{bmatrix}, \tag{4}$$

where P_k is the estimation error covariance of the original model state x_k. The dimension of the augmented state vector is as follows:

$$L^a = L_\mathrm{x} + L_\mathrm{w} + L_\mathrm{v}, \tag{5}$$

where L_x is the original state dimension, L_w is the process noise dimension, and L_v is the measurement noise dimension (i.e., $\mathrm{x}_k^a \in \mathbb{R}^{L_\mathrm{x}+L_\mathrm{w}+L_\mathrm{v}}$).

a. Sigma point selection

During this phase, $2L^a + 1$ sigma points are deterministically chosen using the SUT to enable them to capture the statistical properties of the nonlinear model (Julier et al. 2000; Ito and Xiong 2000; Wan and van der Merwe 2000). Thus,

$$\chi_{k-1|k-1}^0 = \hat{\mathrm{x}}_{k-1|k-1}^a, \tag{6}$$
$$\chi_{k-1|k-1}^i = \hat{\mathrm{x}}_{k-1|k-1}^a + \left(\sqrt{(L^a+\lambda)P_{k-1|k-1}^a}\right)_i \text{ for } i = 1, \dots, L^a, \text{ and} \tag{7}$$
$$\chi_{k-1|k-1}^i = \hat{\mathrm{x}}_{k-1|k-1}^a - \left(\sqrt{(L^a+\lambda)P_{k-1|k-1}^a}\right)_i \text{ for } i = L^a+1, \dots, 2L^a, \tag{8}$$

where the subscript $k-1|k-1$ means the posterior or analysis state at time $k-1$, λ is a scaling parameter, and $\left(\sqrt{(L+\lambda)P_{k-1|k-1}^a}\right)_i$ is the ith column (or row) vector of the matrix square root of the weighted covariance matrix $(L+\lambda)P_{k-1|k-1}^a$. The weight associated with the ith sigma-point is defined as

$$\omega_{(m)}^0 = \frac{\lambda}{L^a+\lambda}, \tag{9}$$
$$\omega_{(c)}^0 = \frac{\lambda}{L^a+\lambda} + (1-\alpha^2+\beta), \text{ and} \tag{10}$$
$$\omega_{(m)}^i = \omega_{(c)}^i = \frac{1}{2(L^a+\lambda)} \text{ for } i = 1, \dots, 2L^a, \tag{11}$$

where $\omega_{(m)}^i$ and $\omega_{(c)}^i$ represent the weighting terms used to calculate the mean and covariance, respectively. More detailed derivations of the scaling parameter λ α κ, and β can be found in Van Der Merwe, R. (2004).

b. Mean and covariance estimation

The sigma points are propagated through the fully nonlinear system [Eqs. (1) and (2)], while making no assumptions regarding the linearity of prediction and observation models.

$$\chi_{(\mathrm{x}),k|k-1}^i = f\left(\chi_{(\mathrm{x}),k-1|k-1}^i, \chi_{(\mathrm{w}),k-1|k-1}^i\right) \text{ for } i = 0, \dots, 2L^a, \tag{12}$$
$$\mathrm{z}_k^i = h\left(\chi_{(\mathrm{x}),k|k-1}^i, \chi_{(\mathrm{v}),k-1|k-1}^i\right) \text{ for } i = 0, \dots, 2L^a, \tag{13}$$

where $\chi_{(\mathrm{x}),k|k-1}^i$ is the forecast sigma point state vector at time k, $\chi_{(\mathrm{w}),k-1|k-1}^i$ and $\chi_{(\mathrm{v}),k-1|k-1}^i$ are sigma point vectors that correspond to the model error and observation error respectively, and z_k^i represents the transformed sigma point in observation space. Using the transformed sigma points obtained from Eqs. (12) and (13), the predicted state estimate (background mean) $\hat{\mathrm{x}}_{k|k-1}$, corresponding covariance $P_{k|k-1}$, predicted measurement estimate $\hat{\mathrm{z}}_k$, and its error covariance S_k at time k can then be calculated by

$$\hat{\mathrm{x}}_{k|k-1} = \sum_{i=0}^{2L^a} \omega_{(m)}^i \chi_{(\mathrm{x}),k|k-1}^i, \tag{14}$$
$$P_{k|k-1} = \sum_{i=0}^{2L^a} \omega_{(c)}^i (\chi_{(\mathrm{x}),k|k-1}^i - \hat{\mathrm{x}}_{k|k-1})(\chi_{(\mathrm{x}),k|k-1}^i - \hat{\mathrm{x}}_{k|k-1})^T, \tag{15}$$
$$\hat{\mathrm{z}}_k = \sum_{i=0}^{2L^a} \omega_{(m)}^i \mathrm{z}_k^i, \text{ and} \tag{16}$$
$$S_k = \sum_{i=0}^{2L^a} \omega_{(c)}^i (\mathrm{z}_k^i - \hat{\mathrm{z}}_k)(\mathrm{z}_k^i - \hat{\mathrm{z}}_k)^T. \tag{17}$$

The SPKF expressions for calculating the optimal Kalman gain K_k, the updated state estimate (analysis mean) $\hat{\mathrm{x}}_{k|k}$, and its covariance $P_{k|k}$ are as follows (more detailed derivations for K_k and $P_{k|k}$ can be found in the appendix):

$$K_k = P_{\mathrm{xz}} S_k^{-1}, \tag{18}$$
$$\hat{\mathrm{x}}_{k|k} = \hat{\mathrm{x}}_{k|k-1} + K_k(\mathrm{z}_k - \hat{\mathrm{z}}_k), \text{ and} \tag{19}$$
$$P_{k|k} = P_{k|k-1} - K_k S_k K_k^T, \tag{20}$$

where P_{xz} denotes the cross covariance between $\hat{\mathrm{x}}_{k|k-1}$ and $\hat{\mathrm{z}}_k$ and can be computed by

$$P_{\mathrm{xz}} = \sum_{i=0}^{2L^a} \omega_{(c)}^i (\chi_{(\mathrm{x}),k|k-1}^i - \hat{\mathrm{x}}_{k|k-1})(\mathrm{z}_k^i - \hat{\mathrm{z}}_k)^T. \tag{21}$$

However, the SPKF approach is computationally unfeasible in high-dimensional models, such as atmospheric or ocean models, due to the large dimensionality (L^a) of the augmented states. Another major drawback of the SPKF approach is that the sigma points of the SPKF are determined based on the global domain, making it impossible to use the localization scheme for generating the sigma points, which is a good strategy for overcoming issues with computational feasibility.

LUTKF

The LUTKF algorithm is an implementation of the SPKF that estimates the state of the dynamical system for the specific (but often found) case, where the process and measurement noises are additive (van der Merwe 2004). To illustrate, suppose we have an L-dimensional discrete-time nonlinear system described by the dynamical model and the observation model with additive noise. Accordingly, Eqs. (1) and (2) can be rewritten, respectively, as

$$\mathrm{x}_k = f(\mathrm{x}_{k-1}) + \mathrm{w}_{k-1}, \tag{22}$$
$$\mathrm{z}_k = h(\mathrm{x}_k) + \mathrm{v}_k. \tag{23}$$

In the case of additive process and measurement noises, the system state does not need to be augmented with the random noise variables. The use of the non-augmented state vector can reduce the dimension of the sigma points as well as the total number of sigma points used. While the dimension of the augmented state vector in the SPKF is L^a, the dimension of the state vector in the LUTKF is L_x. Hence, while the number of the sigma points required to estimate the true mean and covariance in the SPKF is $2L^a + 1$, the number of the sigma points used in the LUTKF is $2L_\mathrm{x} + 1$.

a. Non-augmented SPKF filtering

The sigma point selection and state estimation of the LUTKF are similar to those of the SPKF, except for the use of the non-augmented state vector; that is, the augmented state estimate $\hat{\mathrm{x}}^a$, covariance P^a, and state dimension L^a in both phases of the SPKF [Eqs. (6)-(21)] are replaced with non-augmented forms $\hat{\mathrm{x}}$, P, and L_x for the LUTKF, respectively. Furthermore, the sigma points are transformed through the dynamical model (22) and measurement model (23) as follows:

$$\chi_{k|k-1}^i = f\left(\chi_{k-1|k-1}^i\right) \text{ for } i = 0, \dots, 2L_\mathrm{x}, \tag{24}$$
$$\mathrm{z}_k^i = h\left(\chi_{k|k-1}^i\right) \text{ for } i = 0, \dots, 2L_\mathrm{x}. \tag{25}$$

Note that unlike the SPKF, the covariance matrices Q_{k-1} and R_k are added at the end of the prior error covariance $P_{k|k-1}$ and measurement error covariance S_k, respectively, in order to take account of the model error w_{k-1} and observation noise v_k as follows:

$$P_{k|k-1} = \sum_{i=0}^{2L_\mathrm{x}} \omega_{(c)}^i (\chi_{k|k-1}^i - \hat{\mathrm{x}}_{k|k-1})(\chi_{k|k-1}^i - \hat{\mathrm{x}}_{k|k-1})^T + Q_{k-1}. \tag{26}$$
$$S_k = \sum_{i=0}^{2L_\mathrm{x}} \omega_{(c)}^i (\mathrm{z}_k^i - \hat{\mathrm{z}}_k)(\mathrm{z}_k^i - \hat{\mathrm{z}}_k)^T + R_k. \tag{27}$$

The non-augmented SPKF algorithm has been successfully implemented and employed to analyze practical systems (Farina 2002, Crassidis 2003, Bshara et al. 2010, Cui et al. 2017). A detailed description and deviation of this SPKF algorithm can be found in van der Merwe (2004).

b. Spatial localization

The simplest method for implementing the R localization takes into account the observations only within a cutoff radius surrounding the grid point, and it carries out the analysis separately for each spatial grid point of the model (Houtekamer and Mitchell 1998; Keppenne 2000; Ott et al. 2004; Hunt et al. 2007). However, the abrupt cutoff distance in the R localization can lead to a noisy estimate of the model state. To solve this problem, the smoothed R localization was proposed by Hunt et al. (2007). The localization can achieve an effect similar to the B localization by multiplying the elements of the observation error covariance R_k by a function that increases the uncertainty assigned to the observations gradually, as the distances of the observations from the analysis grid point increases (Houtekamer and Zhang 2016).

The localization can be applied to the LUTKF by dividing the diagonal elements of R_k in Eq. (27) by the Gaussian localization function $G(d, L) = \exp(-d^2/2L^2)$, where d is redefined as the distance between observation and analysis grid point, and L is reinterpreted as the localization distance for the observations. In practice, this study uses the following piecewise polynomial approximation of the Gaussian localization function with compact support, which is given by Eq. (4.10) of Gaspari and Cohn (1999).

Simulation on Lorenz-96 Model

- For experiments executed in this study, the L96 model setup is similar to that of Lorenz and Emanuel (1998), where the number of model variables N_x is set to 40 and the magnitude of the forcing F is fixed at 8.
- A localization length scale was set to 1.1 and 3.7 for the LUTKF and LETKF, respectively.
- The tunable parameter for the RTPS method [the α in Eq. (3) of Whitaker and Hamill (2012)] used in the LETKF was set to 0.4 for all the experiments.
- Trial simulations (not shown here) showed that values of $\alpha = 1$, $\beta = 2$, and $\kappa = 0$ lead to a high correlation between the true state and its estimated value by the LUTKF and SPKF in the experiments executed in this study.
- The diagonal elements of error covariance matrix Q and R are set to 0.01.
- 100 observations are created by adding the noise $\mathrm{v} \sim N(0, R)$ to the true data using Eq. (23).

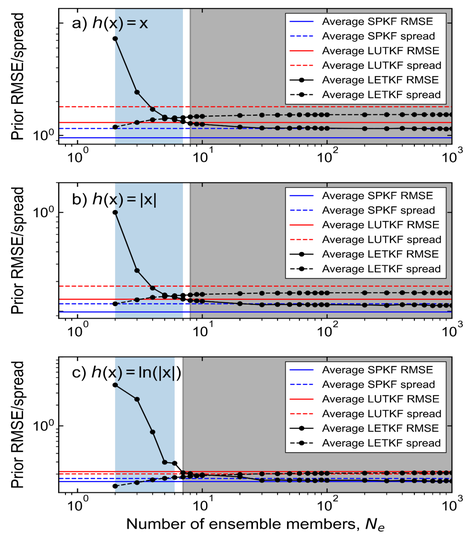

Fig. 1. Prior mean RMSE and spread as a function of ensemble size with respect to the three different observation operators. The blue shading shows that the LUTKF can perform better than the LETKF when small ensembles are used, while the gray shading represents marginal accuracy improvements of LETKF over the LUTKF when enough ensemble sizes are used.

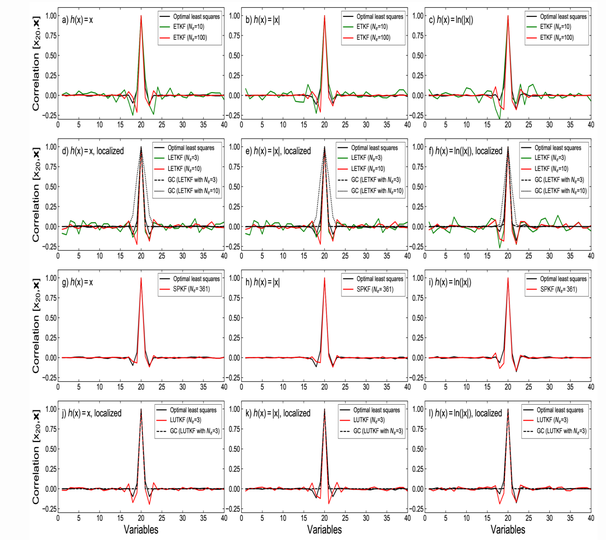

Fig. 2. Prior correlations between state variable 20 and all other variables in the background error covariance, which are estimated using the global filters [(a)-(c) ETKF and (g)-(i) SPKF] and local filters [(d)-(f) LETKF and (j)-(l) LUTKF] for three different types of observations.

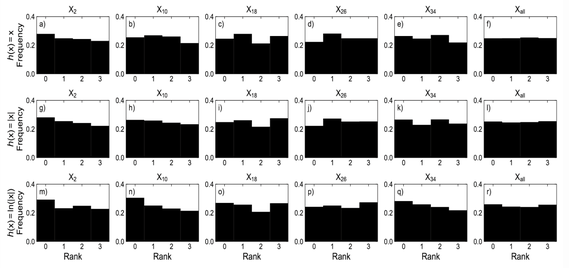

Fig. 3. Rank histogram obtained from prior ensembles of LUTKF using $N_e = 3$ for the three observation types. The verification is carried out for state variables 2, 10, 18, 26, and 34 and for all variables 1-40 (from left to right).

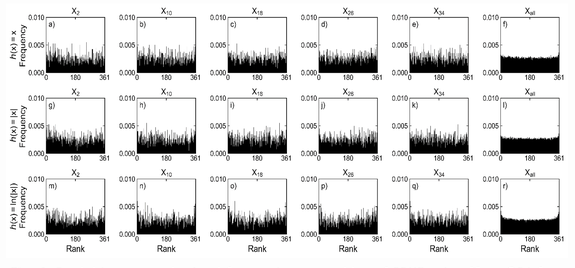

Fig. 4. Rank histogram obtained from prior ensembles of SPKF using $N_e = 381$ for the three measurement operators. The verification is carried out for state variables 2, 10, 18, 26, and 34 and for all variables 1-40 (from left to right).

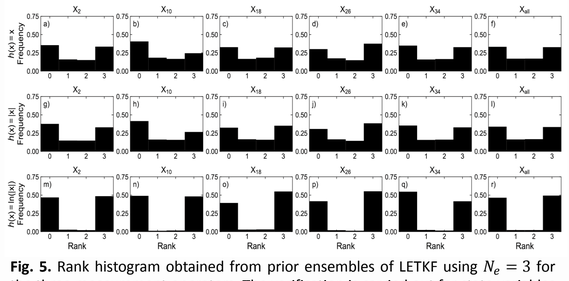

Fig. 5. Rank histogram obtained from prior ensembles of LETKF using $N_e = 3$ for the three measurement operators. The verification is carried out for state variables 2, 10, 18, 26, and 34 and for all variables 1-40 (from left to right).

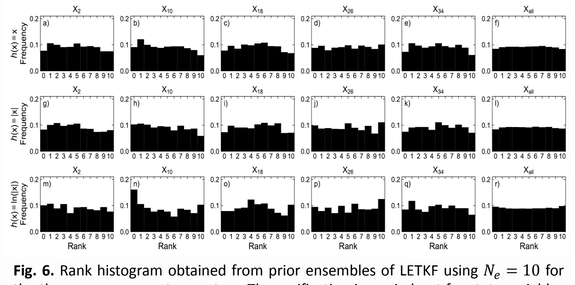

Fig. 6. Rank histogram obtained from prior ensembles of LETKF using $N_e = 10$ for the three measurement operators. The verification is carried out for state variables 2, 10, 18, 26, and 34 and for all variables 1-40 (from left to right).

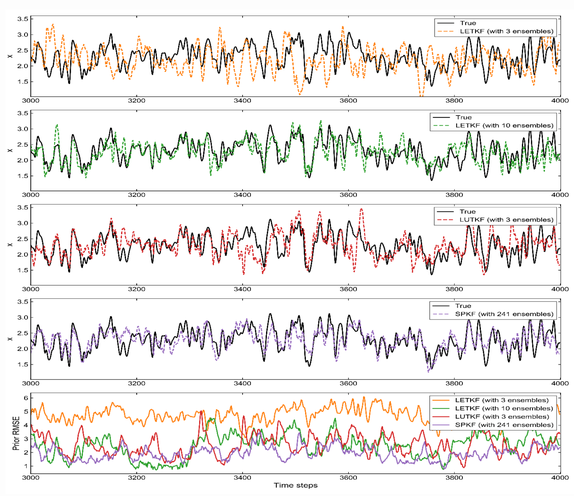

Fig. 7. Case A—(a)-(d) Prior state estimates (dashed curves) and (e) corresponding errors (solid trajectories) for the 40-variable L96 model for $F = 8.0$ and nonlinear observation model h(x) = ln(|x|) with 40 observations and a tenfold increase in the observation noise levels (i.e., R=1.0): (a) LETKF for $N_e = 3$; (b) LETKF for $N_e = 10$; (c) LUTKF for $N_e = 3$; and (d) SPKF for $N_e = 241$.

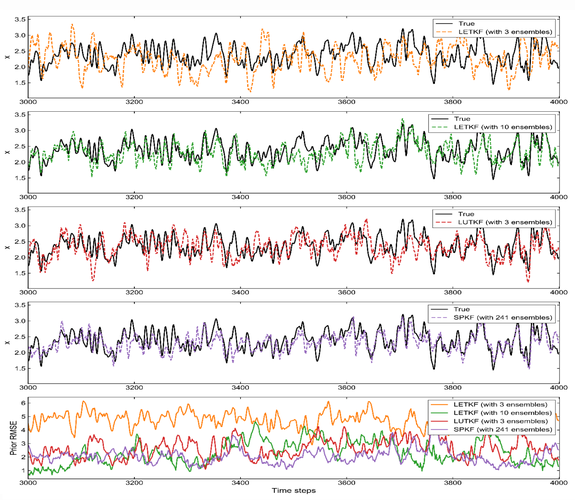

Fig. 8. Case B—(a)-(d) Prior state estimates (dashed curves) and (e) corresponding errors (solid trajectories) for the 40-variable L96 model for $F = 8.1$ and nonlinear observation model h(x) = ln(|x|) with 40 observations and a tenfold increase in the observation noise levels (i.e., R=1.0): (a) LETKF for $N_e = 3$; (b) LETKF for $N_e = 10$; (c) LUTKF for $N_e = 3$; and (d) SPKF for $N_e = 241$.

Table 1. RMSE, correlation, and computational time of each assimilation method for Case A and Case B.

Assimilation method	F=8.0			F=8.1		
	RMSE	Correlation	Computational time (s)	RMSE	Correlation	Computational time (s)
LETKF (using 3 ensembles)	4.712	0.172	3.35	4.785	0.169	3.59
LETKF (using 10 ensembles)	2.369	0.781	4.65	2.483	0.767	4.79
LUTKF (using 3 ensembles)	2.592	0.743	3.83	2.711	0.733	4.00
SPKF (using 241 ensembles)	1.974	0.843	85.81	2.083	0.830	86.63

Summary and Conclusions

We have already begun examining the feasibility of the LUTKF in larger models. Although not discussed in this study, the LUTKF requires a much smaller ensemble size than the LETKF and SPKF to estimate the error statistics of the model in cycling data assimilation experiments carried out with a realistic atmospheric model that includes 70 762 328 variables. Data assimilation experiments using this model will be the topic of a future study that will explore the estimation accuracy, numerical stability, and computational difficulty for high-dimensional problems.